ACS OMEGA

Open Access

http://pubs.acs.org/journal/acsodf

Article

A Hybrid Control Framework for Chemical Processes with Long Time Delay: Theory and Experiments

Antonio Di Teodoro, Marco Herrera, Luis Rincon, Juan J. Gude, and Oscar Camacho*

Cite This: *ACS Omega* 2024, 9, 32469−32480

Read Online

ACCESS | Metrics & More | Article Recommendations

ABSTRACT: This paper proposes a hybrid control framework based on internal model concepts, sliding mode control methodology, and fractional-order calculus theory. As a result, a modified Smith predictor (SP) is proposed for nonlinear systems with significant delays. The particular predictive approach enhances the sliding mode control (SMC) controller's transient responses for dead-time processes, and the SMC gives the predictive structure robustness for model mismatches by combining the previous methods with fractional order concepts; the result is a dynamical sliding mode controller. A numerical example is considered to evaluate the performance of the proposed approach, where a step change, external disturbance, and parametric uncertainty test are performed. A real application in the TCLab Arduino kit is presented; the proposed method presented good performance with a little amount of chattering, and in the disturbance rejection case, the overshoot increased with an aggressive response; in both cases, better tuning parameters can improve the process response and the controller action.

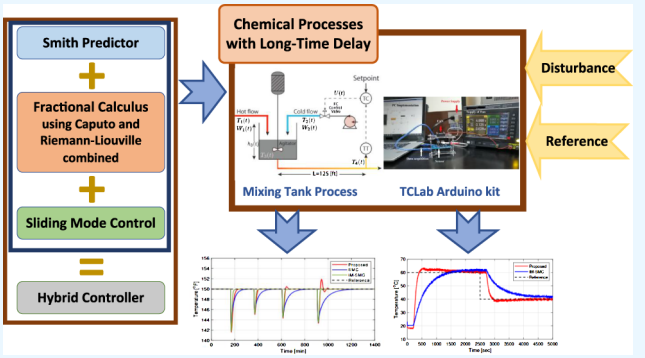

1. INTRODUCTION

Chemical processes, which originated in the petrochemical industry, now have a wide range of applications in biomedicine, the environment, materials, and technology. In particular, they contribute to develop essential medical solutions such as antibiotics and vaccines, and advances in semiconductor materials are critical for modern electronics and computing.[1] These processes can be classified according to purpose, reaction type, and operation mode.[2] The main categories include batch processes utilized in specialty chemical manufacturing, beer brewing, and continuous processes commonly found in oil refining and pharmaceutical production. Catalytic processes are vital in the hydrogenation of ammonia and vegetable oil, while polymerization processes are fundamental in plastic production.[3] Separation processes, including distillation and membrane filtration, are essential for purification.[4] Combustion processes are prevalent in power generation and internal combustion engines. Redox reactions, such as corrosion and electroplating, are significant in various metallurgical and metal-mechanics applications.[5] Lastly, biochemical processes such as fermentation are employed in green industries to produce fuels, chemicals, plastics, pharmaceuticals, and food products.[6] This hierarchical organization provides a structured understanding of the diverse applications of chemical processes in different industries and fields[7,8]

Our primary interest is to investigate control strategies that account for time delays. Dead time is ubiquitous in control applications, and elevated dead time is frequently observed in thermal and other engineering systems, such as chemical, biological, and teleoperation processes.[9] Recently, various approaches have been specifically devised for the control of chemical processes with time delay, which is the main focus of this work.[10−15] The two main origins of delays are physical and mathematical. The first is caused by the transport of materials or fluids over long distances, the processing of measurements with measurement devices, and the actuation of the final control elements. The second is caused by order compensation in high-order systems represented by low-order models.[16] As a result, dead times result in late disturbance detection and lower stability margins of the control system.[17] Therefore, time delays significantly increase the complexity of system analysis and control.[18]

A dead-time compensator (DTC) is a control structure with an internal model that can deal with long dead times. In the

Received: December 30, 2023
Revised: July 5, 2024
Accepted: July 10, 2024
Published: July 20, 2024

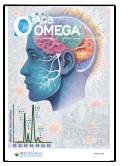

literature, the DTC was called the Smith predictor (SP); see, e.g., refs[17,18]. DTCs are now integrated into control systems as standard modules.[18] The DTC structural design of a control system requires explicit or implicit use of a process model. Unavoidable modeling mistakes result in a mismatch between the model and the actual plant. Consequently, the controller designed for a given model may operate significantly differently when deployed in the actual process, imposing severe limitations on its attainable performance. The development of controllers capable of handling model-plant mismatches is one solution to this challenge.[16,18,19]

The sliding mode control (SMC) methodology, commonly referred to as variable structure control (VSC), is a nonlinear model-based control method.[20] The design of the SMC consists of two phases. In the initial phase, a customized surface must be designed. While on the sliding surface, the plant's dynamics is constrained to the surface's equations and are robust to plant uncertainty and external perturbations. In the second stage, a feedback control rule is developed to ensure convergence of the trajectory of a sliding system;[21] therefore, the sliding surface must be achieved in a finite amount of time.

There has been a growing interest in fractional calculus as a powerful tool for more precise modeling of real-world processes in recent years. Fractional calculus is a mathematical analysis tool used to study integrals and derivatives of arbitrary order, including fractional and real. Fractional derivatives and integrals accurately describe and model many real-world phenomena in systems and various situations.[22,23] In recent decades, fractional integrals and derivatives have been used in various scientific contexts. Using fractional calculus to design control systems results in more robust controllers than controllers of integer order.[24]

Consequently, differential equations based on fractional-order calculus (FOC) are broader mathematical tools than integer-order equations.[25] This is because fractional calculus-based differential equations employ a real-valued derivative or integration operator instead of simply depending on an integer-valued differentiator or integrator. Therefore, the application of fractional-order models to real industrial control problems is expected to positively impact industrial processes in terms of improved performance.

Fractional-order sliding mode control (FOSMC) has recently found many applications in integer-order systems. Machado et al.[26] conducted pioneering work on fractional variable structure controllers and implemented the method on a mechanical manipulator. Aghababa et al.[27] proposed a fractional integral type sliding surface and employed a fractional SMC to stabilize indeterminate fractional-order chaotic systems with model uncertainties and external disturbances. Delavari et al.[28] designed a sliding surface proportional to the derivative and a fuzzy fractional-order sliding mode controller for nonlinear systems.[29] introduced an adaptive fuzzy FOSMC for a high-performance servo-actuation system subject to aerodynamic stresses and uncertainties. Qing et al.[30] studied the problem of stabilizing a class of nonautonomous nonlinear systems. As an illustration, the method was used as a fractional guidance law with an impact angle constraint for a maneuvering target. The simulation results demonstrated the applicability and efficiency of the proposed method.

The use of FOSMC in chemical processes is still a relatively new area of research. However, previous studies suggest that FOSMC is a promising control technique. Several studies have investigated the use of FOSMC for chemical processes. In general, these studies have shown that FOSMC can improve the performance and robustness of control systems for chemical processes; from them, we can highlight.[31−36] Therefore, the future of FOSMC for chemical processes is promising, and it is becoming a more widely used control technique for chemical processes as the theory of fractional calculus and sliding mode control continues to develop.

This paper aims to establish a framework that merges the internal model control structure with sliding mode control methodology and fractional-order calculus theory. As a result, a modified SP is proposed for nonlinear systems with long delays. Therefore, the novel predictive approach improves the transient response of the SMC controller for dead-time processes, and the SMC gives robustness to the predictive structure for model mismatches. Furthermore, using the fractional reduced-order model of the actual process allows us to synthesize the controller law using an equivalent control procedure.[20] Two systems are tested as proof of concept: a nonlinear variable delay system and the TCLab kit.[37]

The contributions of this study can be summarized as follows:

- A generalization of the sliding surface allows for an expression specified as a product of monomials.
- Design of $U_{eq}^{\alpha}(t)$ from the combination of the internal model and the concepts of sliding mode control considering a fractional sliding surface.
- The resulting control law is a dynamical sliding mode control with its respective stability test.
- Applicability to a laboratory prototype and to obtain information on practical issues related to its implementation.

To our knowledge, it is the first time that the concepts of fractional calculus have been used in the hybrid proposed controller approach. The resulting approach conducts a dynamic sliding mode controller (DSMC) design to provide a better transient and steady-state response without affecting the robustness of the controller.

This document is organized as follows. Section 2 presents the theoretical background, including the control fundamentals, definitions, and properties of fractional calculus necessary to develop this work. The synthesis of the controller starting from a fractional reduced-order model of the real process is presented in Section 3. In Section 4, some aspects of the stability of the controller are discussed. The results of two numerical examples and the experimental results are shown in Section 5 to analyze the performance of the proposed controller. Finally, conclusions are drawn in Section 6.

2. BACKGROUND

This section is divided into two subsections. First, several fundamental concepts about control are discussed, and then, in the second, fractional calculus basics are included.

2.1. Control Fundamentals. *2.1.1. Dead-Time Compensator.* The classical structure of SP presented consists of two parts: the first is the controller, which is usually of PID type. However, there is the possibility of designing more robust controllers.[38] On the other hand, there is a prediction phase composed of the process model without dead time. Thus, controller tuning should be performed on this model.[17]

https://doi.org/10.1021/acsomega.3c10514
ACS Omega 2024, 9, 32469−32480

The block diagram for the original SP is shown in Figure 1, where $G_C(s)$ is the transfer function of the controller, usually a PI or PID controller.[18] $G_P(s)$ corresponds to the process being controlled.

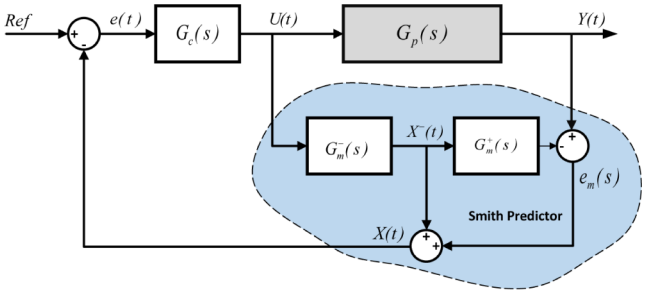

Figure 1. Smith predictor scheme.

The parallel connection to $G_P(s)$, is a reduced-order model representation of the plant that can be described as a first-order plus dead-time (FOPDT) model of the process divided into two parts, $G_m^-(s)$ and $G_m^+(s)$, respectively. The first corresponds to the dynamic part of the model that is fed back to the controller; this part is dead-time free. The second part corresponds to the delay part. However, the model is not perfect, so a feedback signal $e_m(s)$ corresponds to the difference between the process and the output of the model and is used as a correction.

2.1.2. Sliding Mode Control. The SMC is a controller of variable structure created utilizing nonlinear control techniques. It is a robust control that reacts appropriately to nonlinear systems working under unknown conditions. It is also immune to changes in modeling parameters. The SMC design process entails two fundamental phases:

- Stable Sliding Surface Formulation: The initial step involves formulating a Lyapunov-stabilized sliding surface that serves as a specific trajectory. The choice of this sliding surface is a critical decision, dependent upon the system's inherent dynamics and the stipulated control objectives.
- Feedback Control Law Synthesis: A feedback control law is systematically synthesized in the subsequent phase to induce convergence of the system's trajectory toward the aforementioned sliding surface. The control objective is to achieve finite-time convergence, and the motion of the system along this surface is denoted as the *sliding mode*. The resultant feedback controller typically comprises two distinct components:
- High-Frequency Dynamics Controller: This controller component propels the system from its initial state to the sliding surface; this component often employs high-frequency switching dynamics to navigate the system toward the sliding surface expediently.
- Low-Frequency Dynamics Controller: The low-frequency controller assumes control when the sliding surface is reached. This component obliges the process variable to move through the sliding surface to the desired state or trajectory, resulting in stabilization around the desired operating point.

Consequently, the complete SMC design methodology unfolds as follows.

- Selection of a stable sliding surface: Determine a suitable stable Lyapunov sliding surface based on the intrinsic dynamics of the system and the specified control objectives.
- Synthesis of the Feedback Control Law: Systematically design a feedback control law to facilitate the system's trajectory toward the sliding surface and ensure stability.
- Establishment of Convergence Criteria: Ensure that the system achieves the Lyapunov stable sliding surface within a finite time, elucidating the associated convergence criteria and stability conditions.

On the other hand, there are several variations of SMC;[39] in this work, we use one of them, called dynamic sliding mode control (DSMC). Unlike traditional SMC, DSMC incorporates additional dynamics into the system, providing enhanced control performance. One notable advantage of DSMC is its reduced susceptibility to finite-frequency and amplitude oscillations, commonly known as chattering, a drawback associated with the discontinuous function inherent in SMC.[40−42] DSMC achieves this without smoothing functions, ensuring that the controller's performance remains unaffected. This novel control alternative has attracted attention in automatic control engineering, representing a significant improvement over traditional SMC methods.[19,20,43] Continued studies further explore the potential and applicability of DSMC, solidifying its place as an innovative and promising approach in advanced control systems.

Interested readers are encouraged to consult[20,39,44] as key references for a more in-depth understanding of SMC.

2.1.3. Process Model Identification Methods. This section shows the two models used in this work, an integer- and a fractional-order model. The integer order model is the conventional FOPDT model,[45] which is as follows:

$$G_I(s) = \frac{Y(s)}{U(s)} = \frac{Ke^{-t_0 s}}{\tau s + 1} \tag{1}$$

where $K \in \mathbb{R}$ is the process gain, $\tau > 0$ is the time constant, and $t_0 \geq 0$ is the apparent dead-time. This model has been widely used in practice to capture the essential dynamic response of industrial processes for control design.[46]

On the other hand, the fractional-order model considered in this paper is proposed in ref25, which can be viewed as a generalization of the standard FOPDT model.

$$G_F(s) = \frac{Y(s)}{U(s)} = \frac{Ke^{-t_0 s^\beta}}{\tau s^\alpha + 1} \tag{2}$$

with α and $\beta \in \mathbb{R}^+$. The transfer function (eq 2) becomes the fractional first-order plus dead-time (FFOPDT) model for $\beta = 1$.[47]

For this work, the conventional parameters of the FOPDT model are obtained using the reaction curve method.[16] For the FFOPDT case, the parameters will be determined using the method proposed by Gude in ref48 which employs three symmetrical points (25−50−75%) on the process reaction curve. In most cases, the FOPDT and FFOPDT model parameters are close. For the particular test cases, we see that using three asymmetrical points on the reaction curve of the process to determine the FFOPDT model, as proposed in ref49, has a small effect on the parameters. There are other recent identification procedures that are also based on the process reaction curve. The approach proposed in ref50 is

https://doi.org/10.1021/acsomega.3c10514
ACS Omega 2024, 9, 32469−32480

based on the asymptotic property of the Mittag-Leffler function and the hybrid approach described in ref51 combines methods based on the optimization of one variable with the estimation of the remaining model parameters by analytical methods.

2.2. Fractional Calculus. *2.2.1. Definitions of Caputo and Riemann–Liouville Derivative and Their Connection.*

Definition 1. *The Riemann–Liouville fractional integral of order $\alpha > 0$ is given by (see refs22,52−54)*

$$(I_{a^+}^{\alpha}h)(x) = \frac{1}{\Gamma(\alpha)}\int_a^x \frac{h(t)}{(x-t)^{1-\alpha}}dt, \quad x > a \tag{3}$$

We denote by $I_{a^+}^{\alpha}(L_1)$ the class of functions h, represented by the fractional integral (eq 3) of a summable function, that is, $h = I_{a^+}^{\alpha}\varphi$, where $\varphi \in L_1(a,b)$. A description of this class of functions is given in[22,54] ($L_1(a,b)$ space can be defined as a space of measurable functions for which the absolute value is Lebesgue integrable).

Definition 2. *Let $(D_{a^+}^{\alpha}h)(x)$ denote the fractional Riemann–Liouville derivative of order $\alpha > 0$ (see refs22,52−54)*

$$({}_{\mathrm{RL}}D_{a^+}^{\alpha}h)(x) = \left(\frac{d}{dx}\right)^s \frac{1}{\Gamma(s-\alpha)}\int_a^x \frac{h(t)}{(x-t)^{\alpha-s+1}}dt \qquad s = [\alpha]+1,\ x > a, \tag{4}$$

where $[\alpha]$ denotes the integer part of α and Γ is the gamma function. When $0 < \alpha < 1$, then (eq 4) takes the form

$$({}_{\mathrm{RL}}D_{a^+}^{\alpha}h)(x) = \frac{d}{dx}(I_{a^+}^{1-\alpha}h)(x) \tag{5}$$

Example 1.

$${}_{\mathrm{RL}}D_{a^+}^{\alpha}(x-a)^{\gamma} = \begin{cases} 0, & \gamma = \alpha - 1, \\ \dfrac{\Gamma(\gamma+1)}{\Gamma(\gamma-\alpha+1)}(x-a)^{\gamma-\alpha}, & \text{otherwise} \end{cases}$$

with $\alpha \in (0,1)$, $a > 0$, $k \in \mathbb{N}$, and $\gamma > -1$. (See refs54−56)

Definition 3. *Let $\alpha \geq 0$ and $m = [\alpha]$. Then, we can define the operator ${}_cD_{a^+}^{\alpha}$ by ${}_cD_{a^+}^{\alpha}f := I_{a^+}^{m-\alpha}(\frac{d}{dx})^m f$, when $(\frac{d}{dx})^m f \in L_1[a,b]$.*

Example 2. ${}_cD_{a^+}^{\alpha}(x-a)^{\beta} = 0$ *if* $\beta \in \{0, 1, 2, \ldots, m-1\}$.

Lemma 2.1. *Let $\alpha \geq 0$ and $m = [\alpha]+1$. Suppose that f is such that ${}_cD_{a^+}^{\alpha}$ and ${}_{\mathrm{RL}}D_{a^+}^{\alpha}$ exists. Then*

$${}_cD_{a^+}^{\alpha}f = {}_{RL}D_{a^+}^{\alpha}f - \sum_{k=0}^{m-1}\frac{(x-a)^{k-\alpha}}{\Gamma(k-\alpha+1)}\left(\frac{d}{dx}\right)^k f(a)$$

Proof 1. *(See22,53,54)*

consequently, we have the following lemma:

Lemma 2.2. *Let $\alpha \geq 0$ and $m = [\alpha]+1$. Suppose that f is such that ${}_cD_{a^+}^{\alpha}$ and ${}_{\mathrm{RL}}D_{a^+}^{\alpha}$ exists.*

Then ${}_cD_{a^+}^{\alpha}f = {}_{RL}D_{a^+}^{\alpha}f = D_{a^+}^{\alpha}f$. If and only if $(\frac{d}{dx})^k f(a) = 0$ for all $k = 0, \ldots, m-1$.

Proof 2. *As a consequence of the previous lemma*

Other properties connecting both derivatives

Lemma 2.3. *Let $\alpha \geq 0$ and $m = [\alpha]+1$. Suppose that f is such that ${}_cD_{a^+}^{\alpha}$ and ${}_{\mathrm{RL}}D_{a^+}^{\alpha}$ exists*

$${}_{\mathrm{RL}}D_a^{\alpha}\frac{d}{dt}f(t) = \frac{d}{dt}{}_cD_a^{\alpha}f(t)$$

Proof 3. *It follows by direct calculation, using the definitions 1, 2 and 3*

The semigroup property for the composition of fractional derivatives does not hold in general (see ref53). In fact, the property:

$$D_{a^+}^{\alpha}(D_{a^+}^{\gamma}h) = D_{a^+}^{\alpha+\gamma}h \tag{6}$$

holds whenever

$$h^{(j)}(a^+) = 0,\ j = 0, 1, \ldots, s-1 \tag{7}$$

and $h \in AC^{s-1}([a,b])$, $h^{(s)} \in L_1(a,b)$ and $s = [\gamma]+1$ ($AC^s([a,b])$ denotes the class of functions h, which are continuously differentiable on the segment $[a,b]$, up to order $s-1$ and $h^{(s-1)}$ is absolutely continuous on $[a,b]$).

2.2.2. Behavior at the Boundaries 0^+ and 1^-. Consider the real Riemann–Liouville fractional polynomials defined for $\alpha \in (0,1)$ and $a_j^+ > 0$ as (see:[22,54,56,57])

$$\Phi_j^{\alpha,m} := \frac{(x_j - a_j)^{(m+1)\alpha-1}}{\Gamma(\alpha)\Gamma((m+1)\alpha)},\ m \in \mathbb{N}_0,\ j = 0, 1$$

Using the definition 2, (eqs 6 and7). Then we have $[D_{a_j^+}^{\alpha}\Phi_j^{\alpha,m}] = \Phi_j^{\alpha,m-1}$ and:

$$\text{(i)}\ \lim_{\alpha\to 1^-}[D_{a_j^+}^{\alpha}\Phi_j^{\alpha,m}] = \begin{cases} 0, & m = 0, \\ \dfrac{(x_j - a_j)^{m-1}}{(m-1)!}, & m \neq 0. \end{cases}$$

$$\text{(ii)}\ \lim_{\alpha\to 0^+}[D_{a_j^+}^{\alpha}\Phi_j^{\alpha,m}] = 0.$$

Remark 1. *Note that in this example, polynomials act by decreasing the degree and play the role of a constant in this derivative.*

In order to guarantee the stability the systems, we will make use of the two-parameter Mittag-Leffler function. This function is defined classically as

Definition 4. *Let $z \in \mathbb{C}$ and $\alpha > 0$. The two-parameter Mittag-Leffler function is given by*

$$E_{\alpha,\beta}(z) = \sum_{k=0}^{+\infty}\frac{z^k}{\Gamma(\alpha k+\beta)},\ \forall\ z \in \mathbb{C} \tag{8}$$

Remark 2. *Note that $E_{\alpha,\beta}(z) > 0$ for all $z \in \mathbb{C}^+$ and when $\beta = 1$, then $E_{\alpha,\beta}(z) = E_{\alpha}(z)$. This function is uniformly convergent over $\mathbb{C}$ (see22,53,54,58)*

2.2.3. Laplace Transform of Fractional Derivatives.

Definition 5. *The Laplace integral transform of Riemann–Liouville and Caputo fractional derivative of order $\alpha \in (n1,n]$, $n \in \mathbb{N}$ is given by (see22,53):*

$$(\mathcal{L}_{RL}D_{0^+}^{\alpha}f)(s) = s^{\alpha}F(s) - \sum_{j=1}^{n}({}_{\mathrm{RL}}D_{0^+}^{\alpha-j}f)(0^+)s^{j-1}$$

$$(\mathcal{L}_cD_{0^+}^{\alpha}f)(s) = s^{\alpha}F(s) - \sum_{j=0}^{l-1}f^{(j)}(0^+)s^{\alpha-j-1}$$

https://doi.org/10.1021/acsomega.3c10514
ACS Omega 2024, 9, 32469−32480

where $F(s) := \mathcal{L}\{f(t)\}$ *represents the Laplace transform of the function* f, $l = [\alpha]$ *and* $f^{(j)}(0^+) = \frac{d^j}{dt^j} f(t)|_{t\to 0^+}$, $j = 0,\cdots,l-1$. *If* $\alpha \in (0,1)$ *then*

$$(\mathcal{L}_c D_{0^+}^{\alpha} f)(s) = s^{\alpha} F(s) - f(0^+)s^{\alpha-1} \tag{9}$$

and if $\alpha \in (1,2)$ *then*

$$(\mathcal{L}_c D_{0^+}^{\alpha} f)(s) = s^{\alpha} F(s) - f(0^+)s^{\alpha-1} - f'(0^+)s^{\alpha-2} \tag{10}$$

3. CONTROLLER SYNTHESIS

This section presents the controller design. As can be seen in Figure 2, the proposed approach has a fractional dynamical

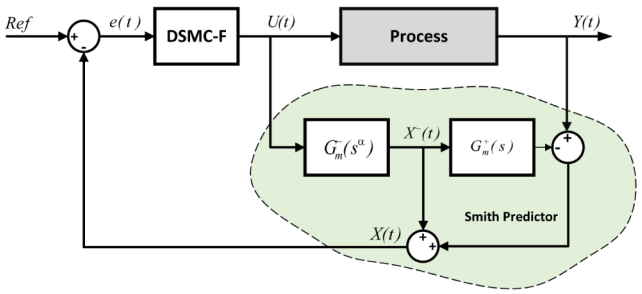

Figure 2. Proposed robust deadtime structure.

sliding mode controller as the main control; therefore, starting from a fractional reduced-order model of the actual process and considering its dead-time-free model part with the SMC procedure, the DSMC-F is obtained.

Different sliding surfaces have been suggested in the literature.[20] A way to obtain the sliding regime that guarantees that the state will advance toward its reference is to use the sliding surface as suggested in refs[21,44].

$$\sigma[e(t)] = \left(\frac{d}{dt} + \lambda\right)^n \int e(t)dt \tag{11}$$

where $\lambda \in \mathbb{R}$, $e(t)$ the difference between the reference $R(t)$ and the controlled variable $X(t)$; $e(t) = R(t) - X(t)$. $\sigma(t)$ is the sliding surface; the designer chooses it, defining the dynamics of the closed-loop system. The objective of the control is to keep the sliding surface at zero. In this paper, we are using a PID surface, where n depends on the order of the system and λ is an adjustable parameter.[21,44]

Remark 3. *We assume that in practical cases, due to the physical nature of the process in Figure 2, the function* $e(t)$ *is a locally integrable function even if the reference is created by a Heaviside type function, and so eq 11 makes sense. This property of* $e(t)$ *is critical in practical applications of the integral and fractional control laws.*

For example, when $n = 2$, then (eq 11) becomes the following equation:

$$\sigma[e(t)] = \left(\frac{d^2}{dt^2} + \lambda_1\frac{d}{dt} + \lambda_0\right)\int e(t)dt \tag{12}$$

with this idea, we can define the following fractional sliding surface version:

Definition 6. *Let* $\alpha, \beta \in \mathbb{R}$, $m = [\alpha + \beta]$, $e(t) \in AC^{m-1}([a, b])$ *and* $e^{(m)} \in L_1(a, b)$. *Then, the fractional sliding surface,* $\sigma_{\alpha,\beta}$, *is defined as*

$$(\sigma_{\alpha,\beta}e)(t) = (D_{0^+}^{\alpha+\beta} + \lambda_1 D_{0^+}^{\alpha} + \lambda_2 D_{0^+}^{\beta} + \lambda_0)(I^1 e)(t) \tag{13}$$

where $\lambda_0, \lambda_1, \lambda_2 \in \mathbb{R}$ *and* $I^1 e(t) = \int e(t)dt$

In general, the fractional sliding surface version is given by

Definition 7. *Let* $\alpha_i \in \mathbb{R}$, $m = [\alpha + \beta]$, $e(t) \in AC^{m-1}([a, b])$ *and* $e^{(m)} \in L_1(a, b)$. *Then, the general form for a fractional sliding surface,* $S_{\alpha,\beta}$, *is defined as*

$$(\sigma_{\alpha,\beta}e)(t) = \left(\sum_{i=0}^{m} \lambda_i D_{0^+}^{\alpha_i^+}\right)(I^1 e)(t) \tag{14}$$

such that $\lambda_0 D_{0^+}^{\alpha_0^+} f = \lambda_0 f$ *and* $\lambda_i \in \mathbb{R}$, *for* $i = 0, ..., m$

From Figure 2, the model for design purposes is as follows:

Definition 8. *Let* $P(s)$ *be a function where* $\alpha \in$ (a,b) *such that*

$$P(s) = \frac{X^-(s)}{U(s)} = \frac{K}{\tau s^{\alpha} + 1} \tag{15}$$

Let $\alpha > 0$ define the fractional transfer function without dead time as

$$[\tau s^{\alpha} + 1]X^-(s) = KU(s) \tag{16}$$

On the one hand, $\alpha \in (0,1]$, then it is possible to use (eq 9) for any inversion in the LHS. On the other hand, if $\alpha \in (1,2]$, the inversion of the first term can be obtained with (eqs 9 and 10) for the following terms. However, if the function X^- satisfies the conditions of Lemmas 1 and 2, then

$$\tau({}_c D_{0^+}^{\alpha} X^-)(t) + X^-(t) = KU(t) \tag{17}$$

Let us define the fractional sliding surface according to (eq 17). We assume the conditions of Lemmas 1 and 2. Let $\alpha > 0$, $m = [\alpha]+1$, $e(t) \in AC^{m-1}([a. b])$ and $e^{(m)} \in L_1(a. b)$. Then, the fractional sliding surface σ_α is defined as

$$\sigma_\alpha[e(t)] = \mathrm{e}^-(t) + \lambda \int e(t)dt = \mathrm{e}^-(t) + \lambda I^1 e(t) \tag{18}$$

Remark 4. *In the classical sense, our operator converges* σ_α *to (eq 11) when* $n = 1$ *and* α *approach* 1^- *which means that in the limit process, all classical results that are known are recovered. The binomial theorem can be used to generalize n. Only emphasizing the fractional calculus for parameters of outer intervals* (0, 1) *is much more difficult to compute. Additionally, we can write*

Remark 5. *Note that the conditions of Lemmas 1 and 2 allow us to commute the classical integral operator* I^1 *into the fractional sliding surface operator in (eq 18), that is,*

$$(\lambda_1 D_{0^+}^{\alpha} + \lambda_0)I^1 = I^1(\lambda_1 D_{0^+}^{\alpha} + \lambda_0) \tag{19}$$

We used the result of Remark 4 followed by applying the Fundamental Theorem of Calculus. The following theorem shows how we can construct the equivalent fractional control law U_{eq}^{α}.

Theorem 3.1. *Let* $\alpha > 0$, $t \neq a$, $m = [\alpha] + 1$, $e(t)$, R, $X^- \in AC^{m-1}$ ([a,b]) *and* $R(t)$, $\dot{X}^-(t) \in L_1(a, b)$. *Then, the equivalent fractional control law* $U_{\mathrm{eq}}^{\alpha}(t)$ *based on fractional sliding of the surface is*

$$U_{\mathrm{eq}}^{\alpha}(t) = \frac{\tau}{K}\left[I^1(D_{0^+}^{\alpha}\dot{R}) + \lambda I^1(D_{0^+}^{\alpha}e) + \frac{X^-}{\tau}\right] \tag{20}$$

Proof 4. *Let* $e(t) = R(t) - X(t)$ *and* $\mathrm{e}^-(t) = R(t) - X^-(t)$. *For simplicity we can consider* $D_{0^+}^{\alpha} =_{\mathrm{RL}} D_{0^+}^{\alpha}$. *First, we apply the*

https://doi.org/10.1021/acsomega.3c10514
ACS Omega 2024, 9, 32469−32480

operator $\frac{d}{dt}$ *to the function* $e^{-}(t)$ *to obtain* $\frac{d}{dt}e^{-}(t) = \dot{R} - \dot{X}^{-}$. *Where* $\dot{R} = \frac{dR}{dt}$ *and* $\dot{X}^{-} = \frac{dX^{-}}{dt}$ *and, as a consequence*

$$\dot{\sigma}_{\alpha} = \frac{d\sigma_{\alpha}[e^{-}(t)]}{dt} = \dot{R} - \dot{X}^{-} + \lambda e = 0.$$

We get the following by applying the operator (eq 5) *and lemma 3 to the previous expression.*

$$D_{0^{+}}^{\alpha}\dot{\sigma}_{\alpha} = D_{0^{+}}^{\alpha}\dot{R} - \frac{d}{dt}{}_{c}D_{0^{+}}^{\alpha}\dot{X}^{-} + \lambda D_{0^{+}}^{\alpha}e = 0. \tag{21}$$

From (eq 17), *we can rewrite* (eq 21) *as*

$$D_{0^{+}}^{\alpha}\dot{\sigma}_{\alpha} = D_{0^{+}}^{\alpha}\dot{R} - \frac{1}{\tau}(K\dot{U} - \dot{X}^{-}) + \lambda D_{0^{+}}^{\alpha}e = 0$$

Finally, we obtain the derivative of U and, consequently, the proof of the theorem.

$$\dot{U}_{\mathrm{eq}}^{\alpha}(t) = \frac{1}{K}[\tau(D_{0^{+}}^{\alpha}\dot{R} + \lambda D_{0^{+}}^{\alpha}e) + \dot{X}^{-}] \tag{22}$$

Remark 6. *If* $R: \mathbb{R} \to \mathbb{R}$ *such that* $R = c$, *where* $c \in \mathbb{R}$. *Then* $\alpha = 0$ *and, consequently,* $D_{a^{+}}^{\alpha}\dot{R} = 0$.

The derivatives of the reference value can be ignored in[21] without affecting the control performance, which allows a simpler controller.

Once the continuous or equivalent part of the SMC, based on the fractional reduced order, has been obtained, a discontinued part is added to obtain the total fractional order SMC law for the deadtime compensator; it can be represented as follows:

$$U^{\alpha}(t) = \int \dot{U}_{eq(t)}^{\alpha}dt + \int \dot{U}_{D(t)}dt \tag{23}$$

Then,

$$U^{\alpha}(t) = U_{\mathrm{eq}}^{\alpha}(t) + K_{D}I^{1}(\mathrm{sign}(\sigma_{\alpha}(t)) \tag{24}$$

4. STABILITY ANALYSIS OF CONTROLLER

In this section, we use the Mittag−Leffler stability theorem and we get the asymptotic stability of the corresponding systems.

Theorem 4.1. (See Theorem 5.1 in[59]). *Let* $x = 0$ *be an equilibrium point for the system*

$$D_{0^{+}}^{\alpha}x(t) = f(x(t)),\ t \geq t_{0}$$

where $0 < \alpha \leq 1$ *and* $I \subset \mathbb{R}$ *be a domain containing the origin* $f \in C^{1}(I)$. *Let* $V(t, x(t))$: $[0, \infty) \times I \to \mathbb{R}$ *be a continuously differentiable function and locally Lipschitz with respect to x such that*

i) $A\|x\|^{a} \leq V(t, x(t)) \leq B\|x\|^{b}$

ii) $D_{0^{+}}^{\alpha}V(t, x(t)) \leq -F\|x\|^{ab}$

where $t \geq 0$, $x \in I$, $\alpha \in (0, 1)$, A, B, F, a and b *are arbitrary positive constants. Then* $x = 0$ *is Mittag−Leffler stable. If the assumptions hold globally on* $\mathbb{R}$, *then* $x = 0$ *is globally Mittag−Leffler stable.*

In particular, considering the following function for $\alpha \in (0, 1)$ and $m \in \mathbb{N}_{0}$

$$\Phi^{\alpha,m}: = \frac{(x(t))^{(m+1)\alpha-1}}{\Gamma(\alpha)\Gamma((m+1)\alpha)}$$

note that, this function satisfies: $\Phi^{\alpha,m} = 0$ in $x = 0$, $\Phi^{\alpha,m} = 0$ in $x \geq 0$ and is locally Lipschitz any interval of $\mathbb{R}$. Finally $D_{0^{+}}^{\alpha}\Phi^{\alpha,0} = 0$, see[55−57]). Our candidate of V can be

$$V(t, x(t)) = \Phi^{\alpha,0}E_{\alpha,\alpha}(-\lambda\Phi^{\alpha,0}) \tag{25}$$

where $E_{\alpha,\beta}$ is the Mittag-Leffler function defined in (eq 8).

This function satisfies

(i) $0 < V(t, x(t)) \leq B\|x\|^{b}$ for $x \in I \subset \mathbb{R}$ and any $B \in \mathbb{R}$.

(ii) $D_{0^{+}}^{\alpha}V(t, x(t)) = -\lambda V(t, x(t)) \leq -F\|x\|^{ab}$ for any $F, a, b \in \mathbb{R}$, see ref 22

in consequence, $x = 0$ is Mittag−Leffler stable, using the Remark 4.4 in ref[59] (Mittag−Leffler stability and Generalized Mittag−Leffler stability imply asymptotic stability) we guarantee asymptotic stability of our system.

Example 3. *An explicit and particular form of the function* (eq 26)

$$V(t, x(t)) = \frac{t^{\alpha-1}}{\Gamma(\alpha)^{2}}\left[\frac{1}{\Gamma(\alpha)} - \frac{\lambda}{\Gamma(2\alpha)}\frac{t^{\alpha-1}}{\Gamma(\alpha)^{2}} + \epsilon\right] = (\sigma_{\alpha}(t))^{2\alpha}\Gamma(\alpha)\Gamma((2\alpha)) \tag{26}$$

ϵ *represents the truncation error of the series.*

4.1. Connection Between a Lyapunov Function and the Sliding Surface.

Consider eqs 17 and 20, as following

$$(\tau_{c}D_{0^{+}}^{\alpha} + 1)X^{-}(t) = KU(t)$$

and

$$U_{\mathrm{eq}}^{\alpha}(t) = \frac{\tau}{K}\left[I^{1}(D_{0^{+}}^{\alpha}\dot{R}) + \lambda I^{1}(D_{0^{+}}^{\alpha}e) + \frac{X^{-}}{\tau}\right]$$

On the other hand, using $e^{-}(t) = R(t) - X^{-}(t)$, then we have for $\sigma_{\alpha}[e(t)]$, the expression

$$\sigma_{\alpha}[e(t)] = R - X^{-} + \lambda I^{1}e(t)$$

in consequence:

$${}_{c}D_{0^{+}}^{\alpha}\sigma_{\alpha}[e(t)] = {}_{c}D_{0^{+}}^{\alpha}R - {}_{c}D_{0^{+}}^{\alpha}X^{-} + \lambda I^{1}({}_{c}D_{0^{+}}^{\alpha}e(t))$$

Using lemma 2.3 and algebraic manipulations, we get

$$(\tau_{c}D_{0^{+}}^{\alpha} + 1)X^{-}(t) = \tau\left[{}_{c}D_{0^{+}}^{\alpha}\sigma_{\alpha}[e(t)] - {}_{c}D_{0^{+}}^{\alpha}X^{-} + \frac{X^{-}}{\tau}\right] + U_{D}$$

Then

$${}_{c}D_{0^{+}}^{\alpha}\sigma_{\alpha}[e(t)] = -U_{D}$$

Using lemma 2.3, we obtain that

$$\frac{d}{dt}{}_{c}D_{0^{+}}^{\alpha}\sigma_{\alpha}[e(t)] = D_{0^{+}}^{\alpha}\frac{d}{dt}\sigma_{\alpha}[e(t)] - \frac{d}{dt}U_{D} \tag{27}$$

Finally, as we expect

$$\dot{V} = \lim_{\alpha\to 1} D_{0^{+}}^{\alpha}V < \lim_{\alpha\to 1}(\sigma_{c})(D_{0^{+}}\sigma_{\alpha}) < 0.$$

5. RESULTS

In this section, numerical simulation and experimental examples are presented to analyze the performance of the proposed controller. The first example is a nonlinear mixing tank process, and the experimental results are based on a

https://doi.org/10.1021/acsomega.3c10514
ACS Omega 2024, 9, 32469−32480

thermal system called TCLab. The performance of the proposed controller is measured using the following indices: Integral Absolute Error (IAE), Integral Square Error (ISE), Total Variation of Control Action (TVu), Maximum Overshoot ($MO\%$) and Settling Time (t_s).

5.1. Mixing Tank Process. The mixing tank process is a nonlinear system[21,60] and consists of the simultaneous entry of the hot flow $W_1(t)$ and the cold flow $W_2(t)$ into the process with temperatures $T_1(t)$ and $T_2(t)$, respectively, as shown in Figure 3. The output $T_4(t)$ is the temperature of the mixture

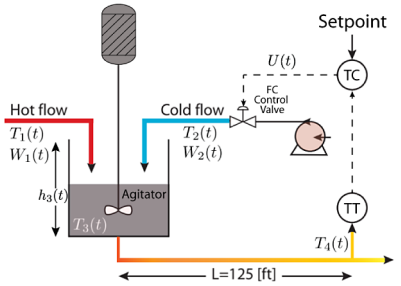

Figure 3. Mixing tank process.

measured at a point 125 ft downstream of the mixing tank. The Fail-Closed (FC) actuator regulates the cold stream to maintain the desired temperature T_3 within the mixing tank.

The transportation lag or delay time[21] is described as follows:

$$t_0 = \frac{LA\rho}{W_1(t) + W_2(t)} \tag{28}$$

where A is the cross-section of the pipe, L the length of the pipe, ρ the density of the contents of the mixing tank and $W_1(t)$ and $W_2(t)$ the variables of the hot and cold inlet flow, respectively.

Taking into account the delay between the tank and the sensor location, T_4 gives the following:

$$T_4(t) = T_3(t - t_0) \tag{29}$$

Since, the delay can change depending on flow values, the tank mixing system is considered a process with variable time delay which is difficult to control.

To determine an approximate model of the nonlinear mixing tank process, the reaction curve identification method is used.[18] From the steady-state values considered as operating points in Table 1, a change of 10% in the input variation $u(t)$ is applied as shown in Figure 4.

Table 1. Steady-State Flow Values of Mixing Tank Process

variable	value	variable	value
W_1	250 lb/min	T_1	250°F
W_2	191.17 lb/min	T_2	50°F
set point	150°F	T_3	150°F

The mixing tank process can be characterized using an approximate FOPDT model estimated by using the reaction curve method as

$$G_I(s) \cong \frac{-0.82e^{-4.206s}}{2.2273s + 1} \tag{30}$$

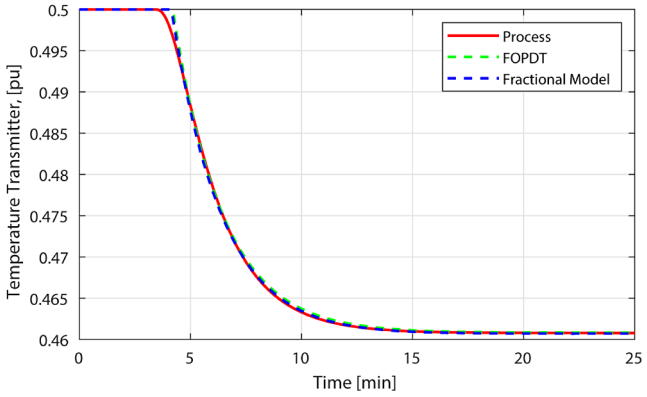

Figure 4. Open loop output response for mixing tank process.

For the fractional model approximation, the method of ref48 is used to obtain the parameters of the FFOPDT model:

$$G_F(s) \cong \frac{-0.82e^{-4.1418s}}{2.2627s^{1.01} + 1} \tag{31}$$

It can be seen that the controllability ratio ($\frac{t_0}{\tau} = 1.83$) corresponds to the difficulty in controlling a process.[45] In addition, it is considered a process with a long time delay.

To validate the approximate models obtained (FOPDT and FFOPDT), the MSE is used, thus $MSE_{\text{FFOPDT}} = 1.5958 \times 10^{-7}$ and $MSE_{\text{FOPDT}} = 2.1405 \times 10^{-7}$. In this case, it can be seen that the FFOPDT model presents a lower MSE value.

The performance of the proposed controller is compared with the IM-SMC controller presented in[61] and the SMC controller presented in.[21] The parameters of the proposed controller are $\lambda = 0.0544$ and $K_D = 0.0001$.

The control objective of the mixing tank process consists in maintaining the measured mixing temperature $T_4(t)$ and $W_2(t)$ despite disturbances in the hot flow $W_1(t)$ and $W_2(t)$.[21] Figure 5a shows the perturbations performed on the hot flow $W_1(t)$

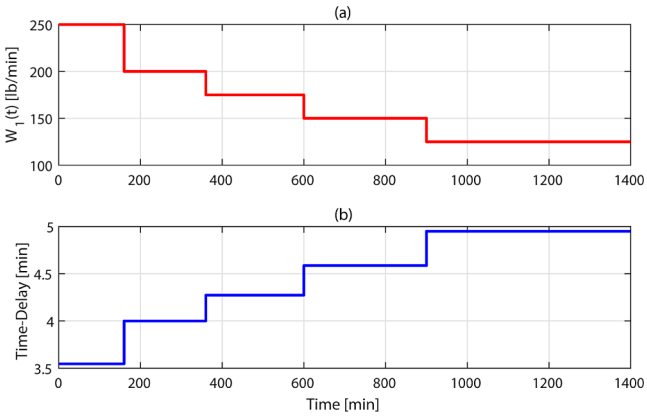

Figure 5. (a) Inlet hot flow variation and (b) time delay variation.

and $W_2(t)$, where four changes of -50 $[lb/min]$ are made at times 160, 360, 600, 900 [sec] respectively. Furthermore, this change in $W_1(t)$ and $W_2(t)$ modifies the time delay from 3.6 to 4.9 [sec], as can be seen in Figure 5b.

Figure 6 shows the closed-loop responses of the mixing tank process to external disturbances, where it can be seen that the three controllers are capable of maintaining the output of the

https://doi.org/10.1021/acsomega.3c10514
ACS Omega 2024, 9, 32469−32480

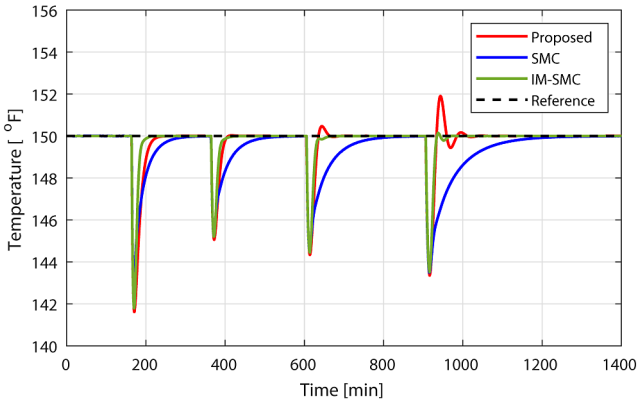

Figure 6. Temperature responses for external disturbance.

process at the desired reference and rejecting the effect of disturbances. Furthermore, for the proposed controller, the process output does not exhibit overshoots in the presence of the first two disturbances. Since our approach adopts a DSMC scheme, it does not incorporate a smoothing function in the discontinuous segment. Consequently, its response tends to be slightly more aggressive than that of the IM-SMC, with an overshoot smaller than 1.5% in the last two disturbances. The IM-SMC experiences a slight performance degradation as the delay increases.

The control actions for the external disturbance test are shown in Figure 7, where it can be seen that the controllers remain within the range allowed by the control action.

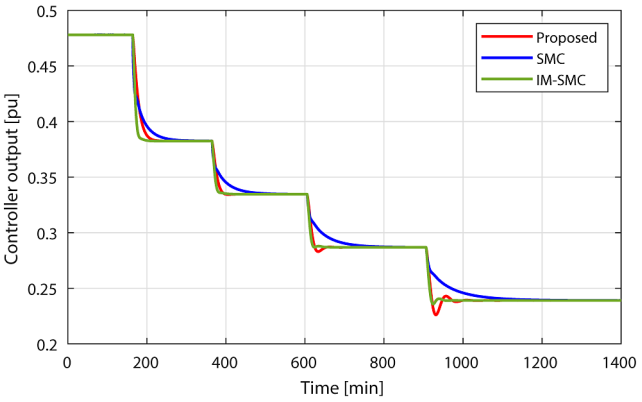

Figure 7. Control actions for external disturbance.

Table 2 shows the performance metrics of the controllers for the external disturbance test. Note that the indices *IAE*, *ISE*, and TV_u are the global values corresponding to the four disturbance tests, while t_s and *MO*% correspond only to the last test. This table shows that the IM-SMC controller presents the lowest values of *IAE*, *ISE*, and *MO*%. In addition, the SMC controller does not present *MO*% but presents the highest values of *IAE*, *ISE*, and t_s. On the other hand, the values of *TVu* are very similar for the three controllers. Finally, although the proposed controller has a value of *MO*% = 1.26, this is very small. Thus, it can be seen that the proposed and the IM-SMC controllers have the best performance results compared to the SMC. It is important to mention that our approach does not have tuning equations, and the little difference compared with the IM-SMC can probably be solved using fine-tuning.

Table 2. Performance Metrics of the Controllers for Mixing Tank Process

controller	IAE	ISE	TVu	*MO*%	t_s [sec]
proposed	5.23	0.23	24.09	1.26	163.5
SMC	9.89	0.30	23.12	0	320
IM-SMC	3.58	0.16	23.61	0.1	82.5

5.2. TCLab Experiments. In this part, a Temperature Control Laboratory (TCLab)[37,40,62] is used for experiments that involve changes in the set point and external disturbances.

The TCLab is handled via a personal computer using a data acquisition system to conduct experimental tests. Furthermore, to carry out the external disturbance test, a fan is placed on top at a distance of 1.5 [cm] from the TCLab, which is connected to a 5 [v] power source, as shown in Figure 8.

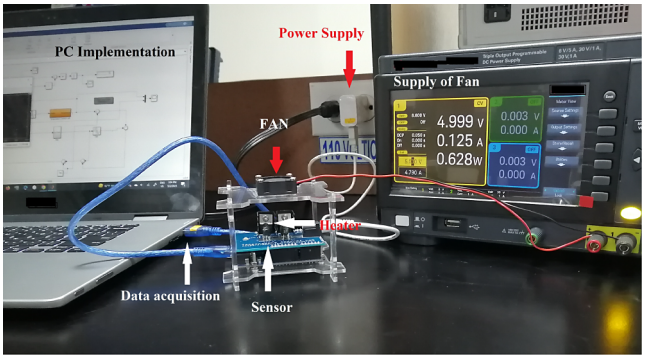

Figure 8. TCLab Experiment test.

The experimental results are performed on Matlab 2019b software on an Intel (R), Core (TM) i7−7500 U @ 2.9 GHz PC, with a sample time of $T_s = 0.1[sec]$.

5.2.1. Model Validation of TCLab Arduino Kit. Since the TCLab Arduino kit does not have a long time delay, the software added an artificial time delay of 200[*sec*]. To obtain an approximate model of the TCLab, the reaction curve-based identification method[46,63] is used, where a change of 40% in the input is applied to the open-loop system, as shown in Figure 9.

The TCLab can be approximated with a FOPDT model by using the reaction curve method as follows:

$$G_I(s) \cong \frac{1.112e^{-222.125s}}{185.771s + 1} \tag{32}$$

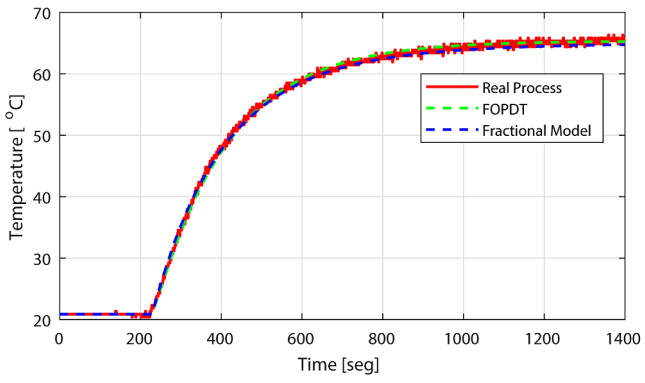

Figure 9. Open loop output response for TCLab process.

https://doi.org/10.1021/acsomega.3c10514
ACS Omega 2024, 9, 32469−32480

For the fractional approximate model, the method[49,50] is used to obtain the parameters of the FFOPDT model:

$$G_F(s) \cong \frac{1.112e^{-220.974s}}{150.8s^{0.9742} + 1} \tag{33}$$

It can be seen that the controllability ratio is $\frac{t_0}{\tau} > 1$. Thus, this process presents a dominant time delay that can be considered difficult to control.

To validate the estimated models, the MSE is used, therefore, $MSE_{\text{FFOPDT}} = 3.2136 \times 10^{-5}$ and $MSE_{\text{FFOPDT}} = 1.034 \times 10^{-4}$. Here, it can be seen that the FFOPDT model presents a lower MSE value.

The performance of the proposed controller is compared with the IM-SMC controller presented in.[61] The parameters of the proposed controller are $\lambda = 0.0123$ and $K_D = 0.1 \times 10^{-6}$

5.2.1.1. Step Change Reference Test. In this part, two reference changes are applied to the system. A temperature change to 60 [°C] is first performed at $t = 0$ [sec] and a reference change to 40 [°C] is second performed at $t = 2500$ [sec], as shown in Figure 10.

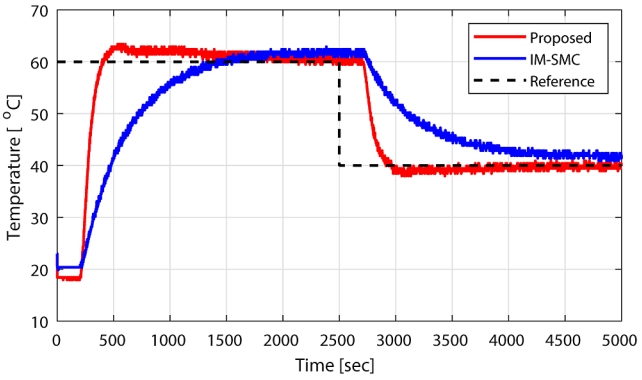

Figure 10. Temperature response for Step change reference test.

The results shown in Figure 10 illustrate a better performance obtained with the proposed method, exhibiting a better settling time than that obtained using the IM-SMC technique. Figure 11 shows the control signal for the step reference change test. Although the control signal of the proposed controller exhibits a slight chattering effect compared to that of the IM-SMC controller, the performance for reference tracking is better in the proposed controller.

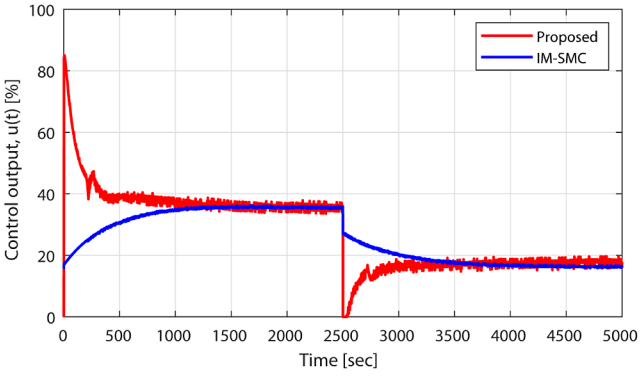

Figure 11. Controller response for Step change reference test.

Table 3 shows the performance metrics for the controllers in the reference changes test. Note that *IAE*, *ISE* and TV_u indices

Table 3. Performance Metrics of the Controllers for Step Change Reference test on TCLab

controller	IAE	ISE	TVu	*MO*%	t_s[*sec*]
proposed	2.15×10^4	7.93×10^6	2.34×10^4	5.66	2156
IM-SMC	8.61×10^5	1.73×10^6	7461	–	–

are the global values corresponding to the two step changes in reference, while t_s and *MO*% correspond only to the first test. In this table, it can be seen that the proposed controller provides the lowest value of *IAE* at the cost of a higher value of TV_u. Observe that the IM-SMC controller is not capable of reaching the reference. Instead, the proposed controller achieves the reference by exhibiting a small overshoot *MO*%.

5.2.1.2. Disturbance Test. In this test, a step change of 60 [°C] is applied in the reference at $t = 0$ [sec]. Then, a disturbance is included in $t = 2500$ [s] during 200[*sec*]. Figure 12 shows a better settling time for the proposed approach, but

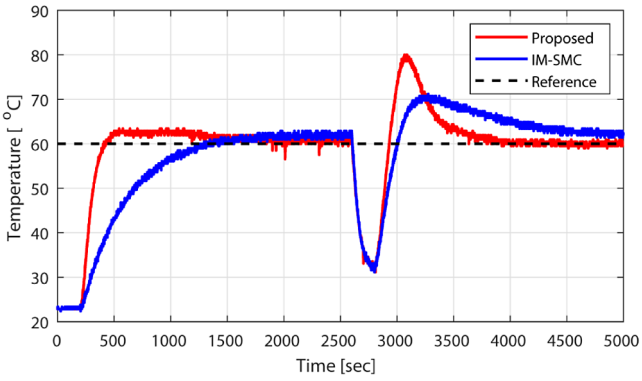

Figure 12. Temperature response for disturbance test.

the overshoot is larger than the IM-SMC. The proposed controller action, which is shown in Figure 13, presents a

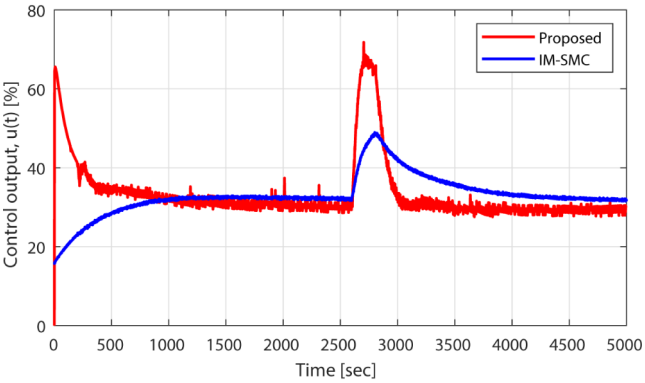

Figure 13. Controller response for disturbance test.

reduced chattering value with more aggressive changes than IM-SMC. In this experiment, some small changes occur around the ambient temperature, and the proposed approach rapidly returns to the set point.

Table 4 shows the performance metrics of each controller for the external disturbance test. It can be seen that the proposed controller presents the lowest value of *IAE* and t_s. In

https://doi.org/10.1021/acsomega.3c10514
ACS Omega 2024, 9, 32469−32480

Table 4. Performance Metrics of the Controllers for Disturbance Test on TCLab

controller	IAE	ISE	TVu	MO%	t_s (sec)
proposed	2.65×10^4	8.22×10^6	2.67×10^4	33.3	1350
IM-SMC	3.95×10^4	1.54×10^6	9288	17.5	-

addition, the IM-SMC controller is not capable of reaching the reference then external disturbance occurs. However, the IM-SMC controller presents a lower value in the ISE index.

6. CONCLUSION

This paper introduced several enhancements. First, a novel control approach was developed by combining the Smith predictor, sliding mode control, and fractional calculus concepts. Additionally, a free dead-time term was incorporated, making controller synthesis simpler. The resulting proposed approach is a fractional-order dynamic sliding mode controller, to our knowledge, for the first time.

Considering performance indicators, the results showed adequate performance in the simulation of the nonlinear example with disturbances and parametric changes compared to other SMC approaches. Furthermore, the approach demonstrated good performance in a real TCLab kit application, involving changes in the set point and external disturbances with minimal chattering. Our controller proposal uses a fractional model in the design, resulting in a dynamic controller. Although the dynamic version of the sliding mode controller effectively reduces chattering, it does not entirely eliminate it; meanwhile, in the IM-SMC case, it employs a smoothing function, a sigmoid one, in the discontinuous part to eliminate chattering.

However, some limitations were also identified. In the disturbance rejection test, a fast response led to a slight increase in overshoot. Improving the tuning parameters, exploring the use of optimization algorithms for this purpose, and adding a set point filter or other methods to reduce the overshoot peaks could enhance the response of the process and the action of the controller.

In summary, the new control approach shows promise by combining several methods and demonstrating good performance, but further tuning is needed to optimize the parameters and improve the response by reducing overshoots. Optimizing fractional parameters is one key to future work.

Finally, this paper balanced mathematical rigor with practical implementation. We are aware that many mathematical details were left out for simplicity, but do not affect the development of the theory or the implementation itself. We continue to work to improve our presentation to achieve the best possible balance.

AUTHOR INFORMATION

Corresponding Author

Oscar Camacho − *Colegio de Ciencias e Ingenierías "El Politécnico", Universidad San Francisco de Quito USFQ, Quito 170157, Ecuador;* orcid.org/0000-0001-8827-5938; Email: ocamacho@usfq.edu.ec

Authors

Antonio Di Teodoro − *Colegio de Ciencias e Ingenierías "El Politécnico", Universidad San Francisco de Quito USFQ, Quito 170157, Ecuador*

Marco Herrera − *Colegio de Ciencias e Ingenierías "El Politécnico", Universidad San Francisco de Quito USFQ, Quito 170157, Ecuador*

Luis Rincon − *Colegio de Ciencias e Ingenierías "El Politécnico", Universidad San Francisco de Quito USFQ, Quito 170157, Ecuador;* orcid.org/0000-0003-4273-1787

Juan J. Gude − *Department of Computing, Electronics and Communication Technologies, Faculty of Engineering, University of Deusto, Bilbao 48007, Spain;* orcid.org/0000-0003-4210-2454

Complete contact information is available at: https://pubs.acs.org/10.1021/acsomega.3c10514

Author Contributions

A.D.T. contributed to Conceptualization, Methodology, Analysis, Writing of Original draft and writing review. M.H. contributed to Conceptualization, Methodology, Analysis, Software. L.R. contributed to Conceptualization, Analysis, Writing original draft, Writing − review, a. J.J.G. contributed to Methodology, Analysis, Software, Writing of original draft, and Writing review. O.C.: contributed to Conceptualization, Methodology, writing of original draft, writing review, Analysis, Editing and Supervision.

Notes

The authors declare no competing financial interest.

ACKNOWLEDGMENTS

This research was supported by the Colegio de Ciencias e Ingenieras, Universidad San Francisco de Quito USFQ, through the Poli-Grants Program under Grant 24280. Marco Herrera thanks the Advanced Control Systems Research Group at USFQ for a research internship. Juan J. Gude thanks the Basque Government for its funding support through the BEREZ-IA Elkartek project (ref KK-2023/00012).

REFERENCES

(1) Herrera, M.; Benítez, D.; Pérez-Pérez, N.; Di Teodoro, A.; Camacho, O. Hybrid controller based on numerical methods for chemical processes with a long time delay. *ACS Omega* **2023**, *8*, 25236−25253.

(2) Dryden, C. E. *Outlines of chemical technology*; Affiliated East-West Press, 1973.

(3) Leach, B. E. Industrial catalysis: Chemistry applied to your lifestyle and environment*Applied Industrial Catalysis* Academic Press 2012,130

(4) Kister, H. Z.; Haas, J. R.; Hart, D. R.; Gill, D. R. *Distillation design*; McGraw-Hill New York, 1992.

(5) Gupta, C. K. *Chemical metallurgy: Principles and practice*; John Wiley & Sons, 2006.

(6) Abramovitz, M. *Biological engineering*; Gale Virtual Reference Library, 2015.

(7) Valencia, R. C. *The future of the chemical industry by 2050*; John Wiley & Sons, 2013.

(8) Sheldon, R. A.; Brady, D. Green chemistry, biocatalysis, and the chemical industry of the future. *ChemSuschem* **2022**, *15*, No. e202102628.

(9) Camacho, O.; Leiva, H. Impulsive semilinear heat equation with delay in control and in state. *Asian J. Control* **2020**, *22*, 1075−1089.

(10) Korupu, V. L.; Muthukumarasamy, M. A comparative study of various Smith predictor configurations for industrial delay processes. *Chem. Prod. Process Model.* **1721**, *17*, 701−732.

(11) Lloyds Raja, G.; Ali, A. New PI-PD controller design strategy for industrial unstable and integrating processes with dead time and inverse response. *J. Control Autom. Electr. Syst.* **2021**, *32*, 266−280.

(12) Kumar, D.; Aryan, P.; Raja, G. L. Design of a novel fractional-order internal model controller-based Smith predictor for integrating processes with large dead-time. *Asia-Pac. J. Chem. Eng.* **2022**, *17*, No. e2724.
(13) Aryan, P.; Raja, G. L. A novel equilibrium optimized double-loop control scheme for unstable and integrating chemical processes involving dead time. *Int. J. Chem. React. Eng.* **2022**, *20*, 1341−1360.
(14) Mehta, U.; Aryan, P.; Raja, G. L. Tri-parametric fractional-order controller design for integrating systems with time delay. *IEEE Trans. Circuits Syst. II* **2023**, *70*, 4166−4170.
(15) Aryan, P.; Raja, G. L.; Vilanova, R. Experimentally verified optimal bi-loop re-located IMC strategy for unstable and integrating systems with dead time. *Int. J. Syst. Sci.* **2023**, *54*, 1531−1549.
(16) Seborg, D. E.; Edgar, T. F.; Mellichamp, D. A.; Doyle, F. J., III. *Process dynamics and control*; John Wiley & Sons, 2016.
(17) Normey-Rico, J. E.; Camacho, E. F. Dead-time compensators: A survey. *Control Eng. Pract.* **2008**, *16*, 407−428.
(18) Liptak, B. G. *Instrument engineers' handbook, volume two: Process control and optimization*; CRC press, 2018.
(19) Proaño, P.; Capito, L.; Rosales, A.; Camacho, O. A dynamical sliding mode control approach for long deadtime systems *2017 4th International Conference on Control, Decision and Information Technologies (CoDIT)* IEEE 2017; 01080113
(20) Utkin, V.; Poznyak, A.; Orlov, Y. V.; Polyakov, A. *Road map for sliding mode control design*; Springer, 2020.
(21) Camacho, O.; Smith, C. A. Sliding mode control: An approach to regulate nonlinear chemical processes. *ISA Trans.* **2000**, *39*, 205−218.
(22) Kilbas, A. A.; Srivastava, H. M.; Trujillo, J. J. *Theory and applications of fractional differential equations*; Elsevier, 2006.
(23) Vazquez, L.; Velasco, M. P.; Usero, D.; Jimenez, S. Fractional calculus as a modeling framework. *Monografias Matematicas Garcia de Galdean* **2018**, *41*, 187−197.
(24) Padula, F.; Visioli, A. *Advances in Robust Fractional Control*; Springer, 2014.
(25) Muresan, C. I.; Ionescu, C. M. Generalization of the FOPDT model for identification and control purposes. *Processes* **2020**, *8*, 682.
(26) Machado, J. T. The effect of fractional order in variable structure control. *Comput. Math. Appl.* **2012**, *64*, 3340−3350.
(27) Aghababa, M. P. A Lyapunov-based control scheme for robust stabilization of fractional chaotic systems. *Nonlinear Dyn.* **2014**, *78*, 2129−2140.
(28) Delavari, H.; Ghaderi, R.; Ranjbar, A.; Momani, S. Fuzzy fractional order sliding mode controller for nonlinear systems. *Commun. Nonlinear Sci. Numer. Simul.* **2010**, *15*, 963−978.
(29) Ullah, N.; Shaoping, W.; Khattak, M. I.; Shafi, M. Fractional order adaptive fuzzy sliding mode controller for a position servo system subjected to aerodynamic loading and nonlinearities. *Aerosp. Sci. Technol.* **2015**, *43*, 381−387.
(30) Qing, W.; Pan, B.; Hou, Y.; Lu, S.; Zhang, W. Fractional-Order Sliding Mode Control Method for a Class of Integer-Order Nonlinear Systems. *Aerospace* **2022**, *9*, 616.
(31) Di Teodoro, A.; Ochoa-Tocachi, D.; Aboukheir, H.; Camacho, O. Sliding-Mode Controller Based on Fractional Order Calculus for Chemical Processes. *2022 IEEE International Conference on Automation/XXV Congress of the Chilean Association of Automatic Control (ICA-ACCA)*. 2022; IEEE 16
(32) Ullah, N.; Mohammad, A. A simulation approach for closed-loop control of coupled four tank system. *Int. J. Model. Simul. Sci. Comput.* **2022**, *13*, 2250029.
(33) Allahem, A.; Karthikeyan, A.; Varadharajan, M.; Rajagopal, K. Computational model of a fractional-order chemical reactor system and its control using adaptive sliding mode control. *Fractals* **2022**, *30*, 2240243−2240287.
(34) Mehri, E.; Tabatabaei, M. Control of quadruple tank process using an adaptive fractional-order sliding mode controller. *J. Control Autom. Electr. Syst.* **2021**, *32*, 605−614.
(35) Haghighi, A.; Ziaratban, R. A non-integer sliding mode controller to stabilize fractional-order nonlinear systems. *Adv. Differ. Equ.* **2020**, *2020*, 1−19.
(36) Ardjal, A.; Bettayeb, M.; Mansouri, R.; Zouak, B. Design and implementation of a Model-Free Fractional Order Intelligent PI Fractional Order Sliding Mode Controller for water level tank system. *ISA Trans.* **2021**, *127*, 501−510.
(37) Mejía, C.; Salazar, E.; Camacho, O. A comparative experimental evaluation of various Smith predictor approaches for a thermal process with large dead time. *Alexandria Eng. J.* **2022**, *61*, 9377−9394.
(38) Báez, E.; Bravo, Y.; Leica, P.; Chávez, D.; Camacho, O. Dynamical sliding mode control for nonlinear systems with variable delay *2017 IEEE 3rd Colombian Conference on Automatic Control (CCAC)* IEEE 2017; 16
(39) Liu, J.; Wang, X.; Liu, J.; Wang, X. *Advanced sliding mode control*; Springer, 2011.
(40) Herrera, M.; Camacho, O.; Leiva, H.; Smith, C. An approach of dynamic sliding mode control for chemical processes. *J. Process Control.* **2020**, *85*, 112−120.
(41) Espín, J.; Estrada, S.; Benítez, D.; Camacho, O. A hybrid sliding mode controller approach for level control in the nuclear power plant steam generators. *Alexandria Eng. J.* **2023**, *64*, 627−644.
(42) Espin, J.; Camacho, C.; Camacho, O. Control of non-self-regulating processes with long time delays using hybrid sliding mode control approaches. *Results Eng.* **2024**, *22*, 102113.
(43) Espín, J.; Castrillon, F.; Leiva, H.; Camacho, O. A modified Smith predictor based−Sliding mode control approach for integrating processes with dead time. *Alexandria Eng. J.* **2022**, *61*, 10119−10137.
(44) Slotine, J.-J. E.; Li, W. *Applied nonlinear control*; Prentice hall: Englewood Cliffs, NJ, 1991.
(45) Åström, K. J.; Hägglund, T. *Advanced PID control*; ISA-The Instrumentation, Systems, and Automation Society Research Triangle Park, 2006; p. 461.
(46) Smith, C. A.; Corripio, A. B. *Principles and practices of automatic process control*; John Wiley & Sons, 2005.
(47) Tavakoli-Kakhki, M.; Haeri, M.; Tavazoei, M. Simple fractional order model structures and their applications in control system design. *Eur. J. Control.* **2010**, *16*, 680−694.
(48) Gude, J. J.; García Bringas, P.; Alomari, M. Influence of the Selection of Reaction Curve's Representative Points on the Accuracy of the Identified Fractional-Order Model. *J. Math.* **2022**, *2022*, 7185131.
(49) Gude, J. J.; García Bringas, P. Proposal of a General Identification Method for Fractional-Order Processes Based on the Process Reaction Curve. *Fractal Fract.* **2022**, *6*, 526.
(50) Gude, J. J.; Di Teodoro, A.; Camacho, O.; García Bringas, P. A new fractional reduced-order model-inspired system identification method for dynamical systems. *IEEE Access* **2023**, *11*, 103214−103231.
(51) Gude, J. J.; García Bringas, P.; Herrera, M.; Rincón, L.; Di Teodoro, A.; Camacho, O. Fractional-order model identification based on the process reaction curve: A unified framework for chemical processes. *Results Eng.* **2024**, *21*, 101757.
(52) Miller, K. S.; Ross, B. *An introduction to the fractional calculus and fractional differential equations*; Wiley, 1993.
(53) Podlubny, I. *Fractional-order systems and fractional-order controllers* Institute of Experimental Physics, Slovak Academy of Sciences Kosice 1994.
(54) Kilbas, A. A.; Marichev, O.; Samko, S. *Fractional integrals and derivatives: Theory and Applications*; Gordon and Breach Science Publishers: Switzerland ; Philadelphia, Pa., USA, 1993.
(55) Ceballos, J.; Coloma, N.; Di Teodoro, A.; Ochoa−Tocachi, D. Generalized Fractional Cauchy−Riemann Operator Associated with the Fractional Cauchy−Riemann Operator. *Adv. Appl. Clifford Algebras* **2020**, *30*, 70.
(56) Ceballos, J.; Coloma, N.; Di Teodoro, A.; Ochoa-Tocachi, D.; Ponce, F. Fractional Multicomplex Polynomials. *Complex Anal. Oper. Theory* **2022**, *16*, 60.

https://doi.org/10.1021/acsomega.3c10514
ACS Omega 2024, 9, 32469−32480

(57) Coloma, N.; Di Teodoro, A.; Ochoa-Tocachi, D.; Ponce, F. Fractional Elementary Bicomplex Functions in the Riemann−Liouville Sense *Adv. Appl. Clifford Algebras* 2021, *31*
(58) Gorenflo, R.; Kilbas, A. A.; Mainardi, F.; Rogosin, S. V. *Mittag-Leffler functions, related topics and applications*; Springer, 2020.
(59) Li, Y.; Chen, Y.; Podlubny, I. Stability of fractional-order nonlinear dynamic systems: Lyapunov direct method and generalized Mittag−Leffler stability. *Comput. Math. Appl.* **2010**, *59*, 1810−1821.
(60) Obando, C.; Rojas, R.; Ulloa, F.; Camacho, O. Dual-Mode Based Sliding Mode Control Approach for Nonlinear Chemical Processes. *ACS Omega* **2023**, *8*, 9511−9525.
(61) Rojas, R.; Camacho, O.; González, L. A sliding mode control proposal for open-loop unstable processes. *ISA Trans.* **2004**, *43*, 243−255.
(62) de Moura Oliveira, P.; Soares, F.; Cardoso, A. Pocket-sized portable labs: Control engineering practice made easy in COVID-19 pandemic times. *IFAC-Papersonline* **2022**, *55*, 150−155.
(63) Alfaro, V. Low-order models identification from the process reaction curve. *Sci. Technol.* **2006**, *24*, 197−216.

https://doi.org/10.1021/acsomega.3c10514
ACS Omega 2024, 9, 32469−32480